

Introduction

Four Issues will be addressed:

- A **Review of the fully implicit solution methods** recently developed for Onetwo. We use a globally convergent Newton solver, supplemented by the (adaptive) method of lines technique to generate solutions to the coupled set of transport equations
- **Benchmarking** the results against Xptor. Both DIII-D and BPX cases were examined.
- A detailed parameter scan of an **ITER-FEAT AT** scenario based on DIII-D experimental data and simulated with the GLF23 confinement model.
- Current and future work, including the installation of the **NTCC Nubeam model** .

METHODS of STIFF CONFINEMENT MODELING and APPLICATION to ITER-FEAT

- Confinement models associated with ITB's are difficult to simulate due to the characteristically stiff behavior encountered. To get well converged solutions requires that new numerical approaches are used to solve the transport equations. The methods presented here **do not rely on space and/or time averaging** !
- Application of these methods to experimental discharges and theoretical modeling of burning plasma experiments has led to new insight and predictions.
- We present results of transport modeling of an ITER-FEAT design based on physics modeling and experimental extrapolation of DIII-D equilibria.

Transport Modeling

$$\underline{\underline{M}} \frac{\partial}{\partial t} \Big|_{\zeta} \underline{u} - \frac{1}{H\rho} \frac{\partial}{\partial \rho} \left(H\rho \underline{\underline{D}} \frac{\partial}{\partial \rho} \underline{u} \right) + \frac{1}{H\rho} \frac{\partial}{\partial \rho} \left(H\rho \underline{\underline{V}} \underline{u} \right) + \underline{\underline{W}} \underline{u} = \underline{S}_{ext} \quad (1)$$

- Here the vector $\underline{u} \equiv [n_1, ..n_N, T_e, T_i, FGHR\rho B_P, \omega]$ represent the dependent variables
- $\underline{\underline{M}}$ is an $N + 4$ by $N + 4$ coefficient matrix with N ion species. For $N = 2$ we have:

$$\mathbf{M} = \begin{pmatrix} 1 & , & 0 & , & 0 & , & 0 & , & 0 & , & 0 \\ 0 & , & 1 & , & \dots & , & 0 & , & 0 & , & 0 \\ \frac{3}{2}T_e \langle Z_1 \rangle & , & \frac{3}{2}T_e \langle Z_N \rangle & , & \frac{3}{2} \left(n_e + T_e \sum n_i \frac{\partial Z_i}{\partial T_e} \right) & , & 0 & , & 0 & , & 0 \\ \frac{3}{2}T + \frac{1}{2} \langle R^2 \rangle \omega^2 m_1 & , & \frac{3}{2}T + \frac{1}{2} \langle R^2 \rangle \omega^2 m_N & , & 0 & , & \frac{3}{2} \sum \langle n_i \rangle & , & 0 & , & \sum m_i \langle n_i R^2 \rangle \omega \\ 0 & , & 0 & , & 0 & , & 0 & , & \frac{1}{FGH^2 \rho^2} & , & 0 \\ \omega m_1 \langle R^2 \rangle & , & \omega m_N \langle R^2 \rangle & , & 0 & , & 0 & , & 0 & , & \sum m_i \langle n_i R^2 \rangle \end{pmatrix}$$

- Matrices $\underline{\underline{D}}$ and $\underline{\underline{V}}$ represent diffusive and convective terms and matrix $\underline{\underline{W}}$ contains the electron ion energy exchange term, written this way for stability of numerical solutions.

Transport Modeling ...

- Discreteization in space results in a set of equations suitable for solution by the **method of lines**:

$$\underline{\underline{M}}_j \frac{\partial \underline{u}_j}{\partial t} - \underline{\underline{P}}_{j-1} \underline{u}_{j-1} - \underline{\underline{Q}}_j \underline{u}_j - \underline{\underline{R}}_{j+1} \underline{u}_{j+1} = \underline{\underline{S}}_{exp,j} \quad (2)$$

- Additional discreteization in time results in a block tri-diagonal system suitable for **globally convergent non linear equation solvers** :

$$\begin{pmatrix} \underline{\underline{B}}_1^{n+\theta} & \underline{\underline{C}}_1^{n+\theta} & 0 & 0 & 0 \\ \underline{\underline{A}}_2^{n+\theta} & \underline{\underline{B}}_2^{n+\theta} & \underline{\underline{C}}_2^{n+\theta} & 0 & 0 \\ 0 & \underline{\underline{A}}_3^{n+\theta} & \underline{\underline{B}}_3^{n+\theta} & \underline{\underline{C}}_3^{n+\theta} & 0 \\ \vdots & \vdots & \vdots & \ddots & \vdots \\ 0 & 0 & 0 & \dots & \underline{\underline{B}}_{n_j}^{n+\theta} \end{pmatrix} \begin{pmatrix} \underline{u}_1^{n+1} \\ \underline{u}_2^{n+1} \\ \underline{u}_3^{n+1} \\ \vdots \\ \underline{u}_{n_j}^{n+1} \end{pmatrix} - \begin{pmatrix} \underline{g}_1^{n+\theta} \\ \underline{g}_2^{n+\theta} \\ \underline{g}_3^{n+\theta} \\ \vdots \\ \underline{g}_{n_j}^{n+\theta} \end{pmatrix} = 0 \quad (3)$$

- Each sub-matrix, $\underline{\underline{A}}, \underline{\underline{B}}, \underline{\underline{C}}$ is $n+4$ by $n+4$, where n is the number of ion species and the 4 comes from the remaining dependent variables (T_e, T, B_P, ω) . The vector \underline{u}_j contains the dependent variables at grid point j and we have assumed a grid of size n_j .
- We allow specification of **different boundary locations for each equation** to perform GLF23 modeling and to aid studies of core edge coupling. The time implicitness parameter $\theta = 1.0$ for these fully implicit methods.

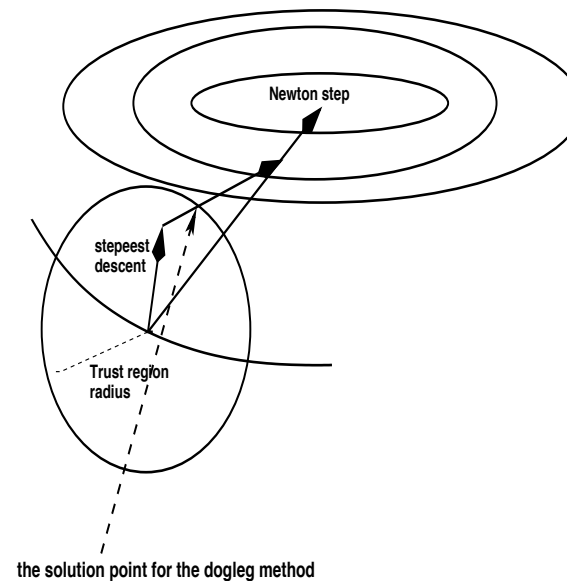
Fully Implicit Solvers

- The best solution method we have found is a **globally convergent Newton method (GCNM)** , that combines steepest descent methods with locally convergent Newton steps and trust region strategies (see St.John,H, aps2001) . The **adaptive method of lines** (as presented in the open source package **RADAU5**), is used sometimes to solve EQS.(2), to confirm GCNM and establish time step scales.
- **Steady state solutions** ,slide ??, can be obtained directly only by using the **GCNM** technique by dropping terms associated with matrix M from matrix B and vector g in EQS(3). This is the only reasonable way we have found to evolve the equations whenever **steady state current drive** is under investigation due to the large time constants involved.

Fully Implicit Solvers Cont.

- We found that no single global strategy will work reliably with confinement models such as GLF23 (which is part of matrix D). Frequently the **adaptive method of lines** will fail with the report that a singular Jacobian was encountered. For the **GCNM** we avoided this problem by perturbation of the Jacobian using the Cholesky decomposition of $J^T J$ to discover the minimal diagonal element required to ensure a positive definite result. Additionally three methods are used in a round robin type approach to generate the solution:

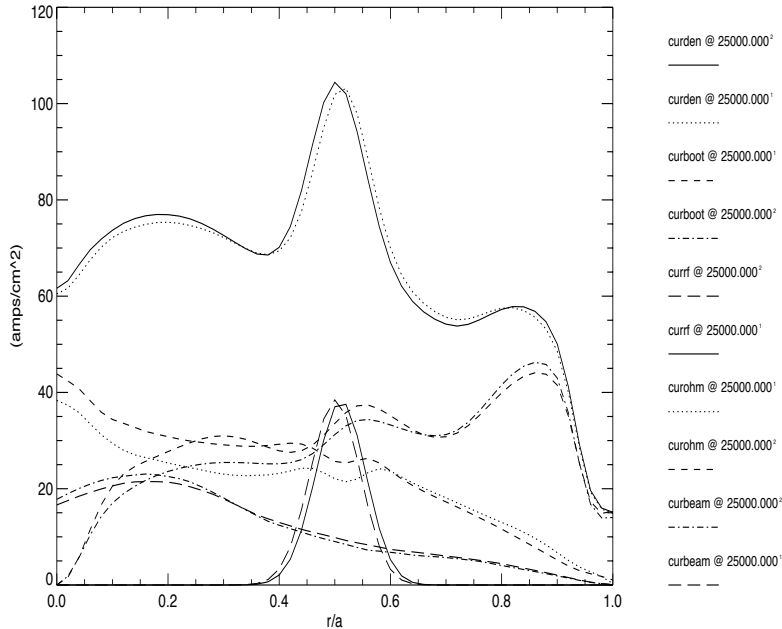
- line search
- and two **trust region methods** which change both the stepsize and direction by using additional information about the local curvature :
 - **dog leg**
 - **hook step**



Example of Steady State Result

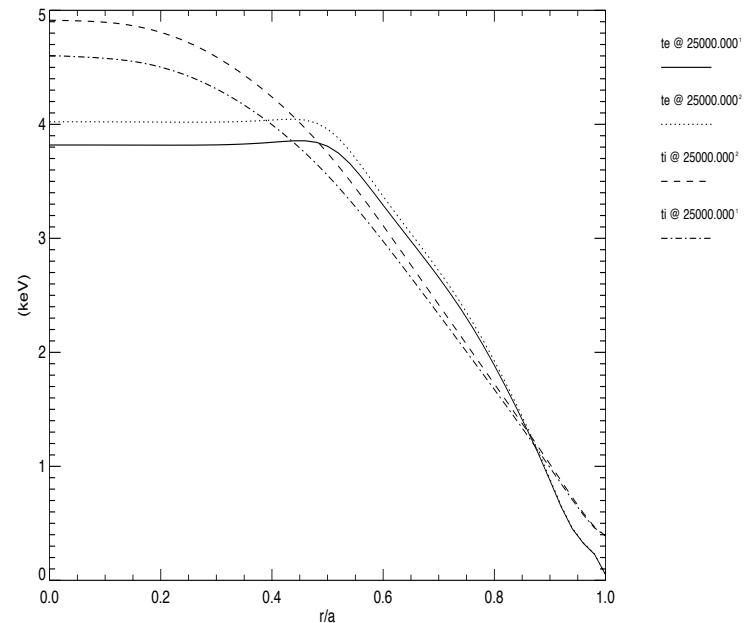
- A major advantage of the fully implicit approach described above is the ability to generate a steady state solution directly. For the usual AT scenario this involves finding quasi stationary profiles for temperatures, densities, poloidal magnetic field and toroidal momentum. This can be done in only a small fraction of the computational time that would be required in a standard approach and makes “what if” type investigations much more accessible.

Steady State Current



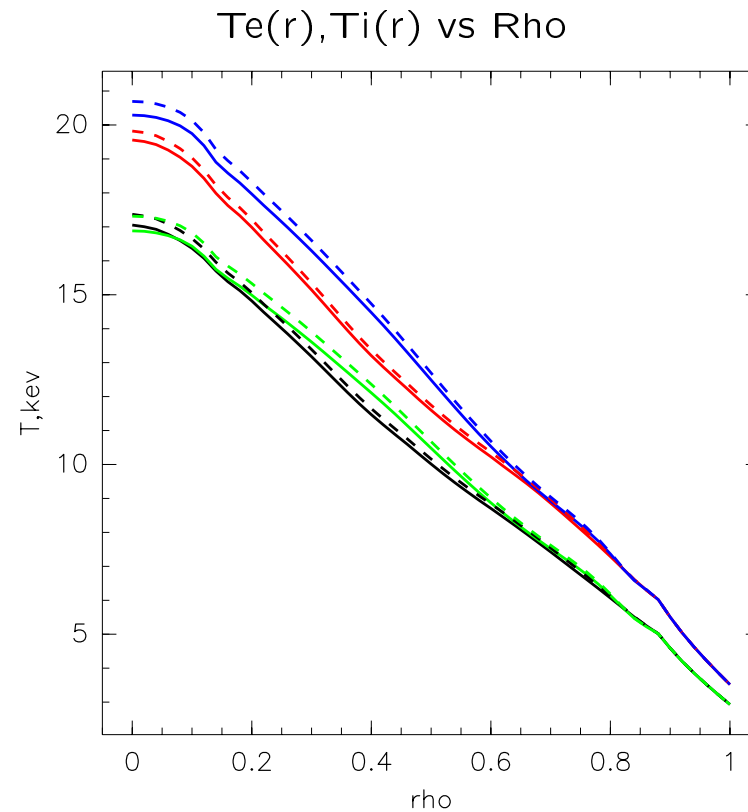
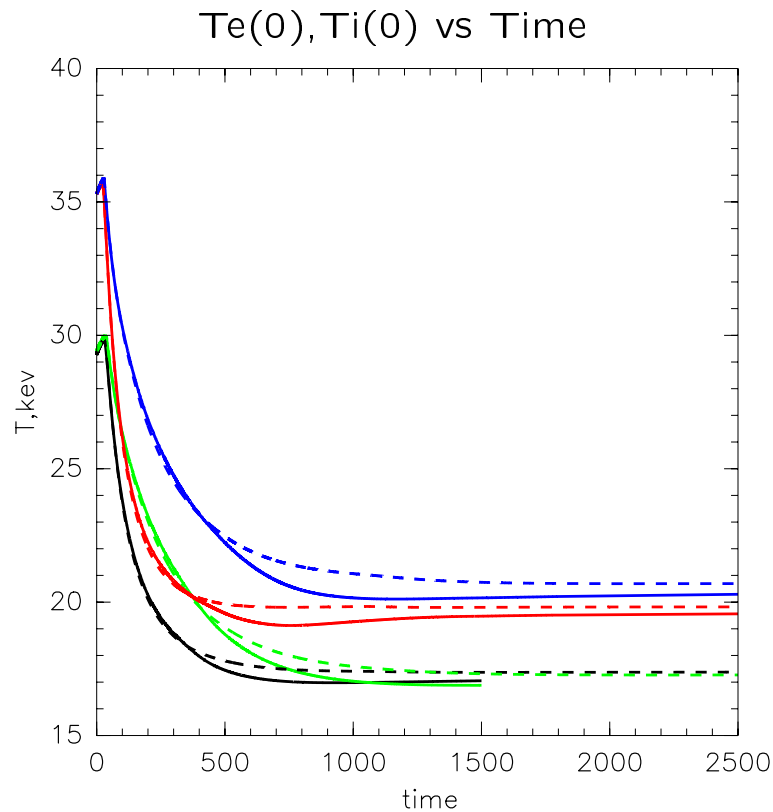
Modeling\john9411\DFD\sauter_110\newton\trplot.nc

TE, Ti with/wo Sawtooth



Modeling\john9411\DFD\sauter_110\newton\trplot.nc

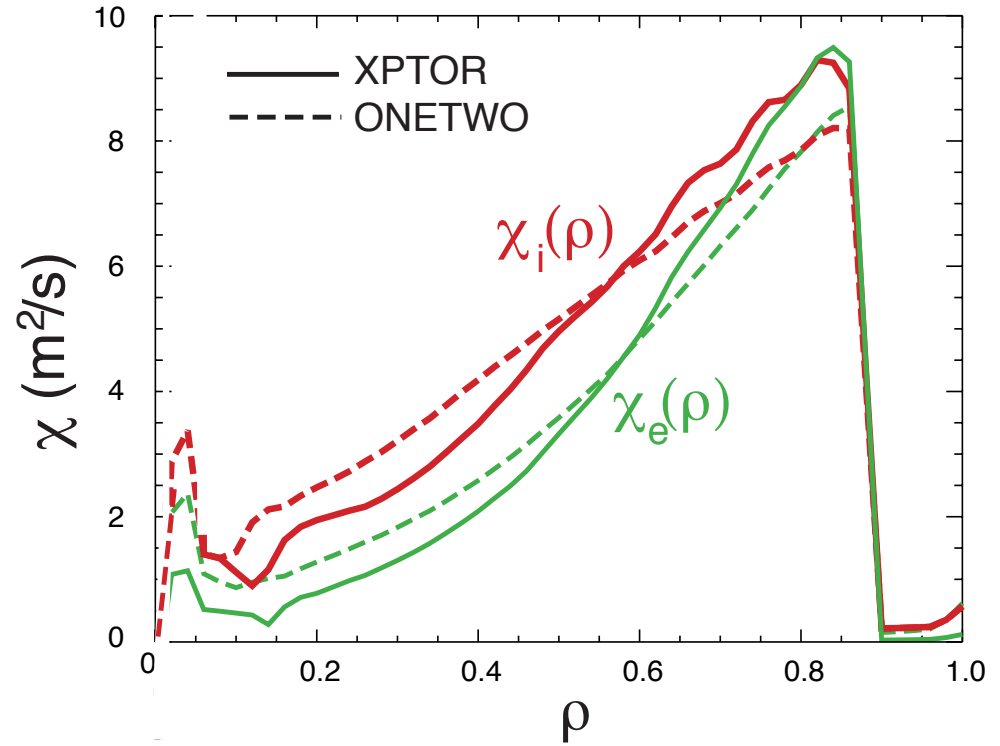
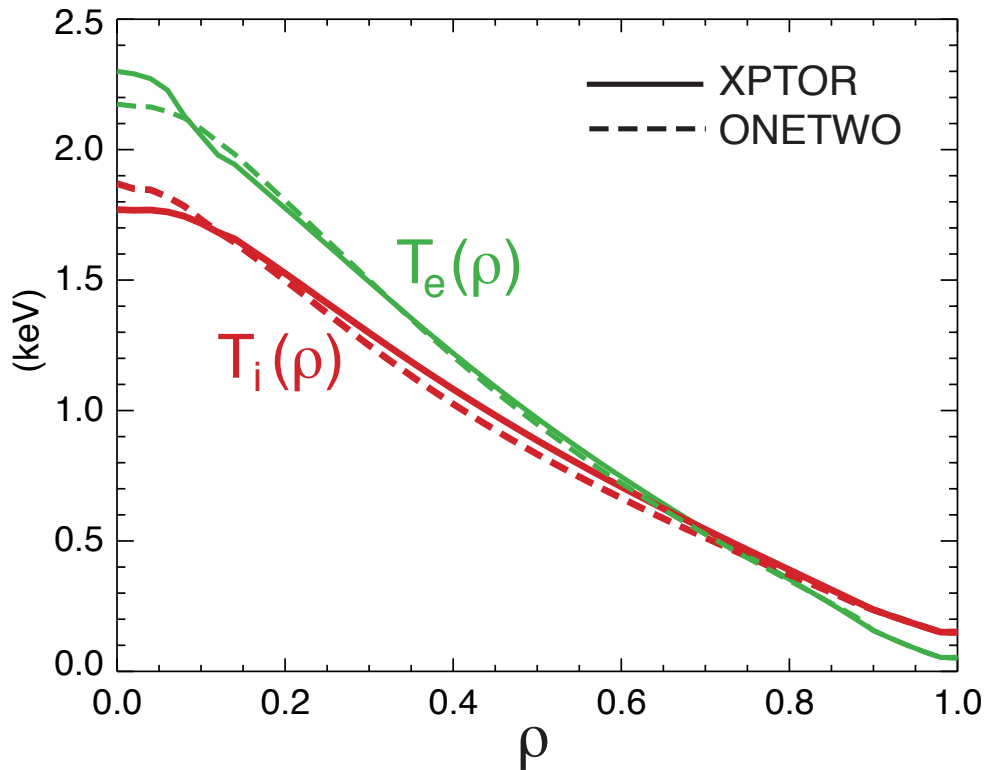
Effects of Time Stepping with GLF23



- Size of time step used to discretize time derivatives in EQ(2) affects solutions. Shown above are the results with $\Delta t = .5$ and $.1$ msec using **GCNM**. The **RADAU5** solution of Eq(3) is similar to the 0.1 msec case shown above but typically takes 50% more time due to the adaptation of the time step as the solution is generated.

Xptor - Onetwo Benchmarks DIII-D and BPX

- The Onetwo calculations were benchmarked against the Xptor results. Typical agreement is demonstrated by DIII-D shot 98777. For more cases see Snowmass ref.



- Results of BPX benchmarking are summarized in Table 1.

Table 1: Xptor - Onetwo Benchmark BPX

Device	Te(0)	Ti(0)	Tped	q0	β_N	Q	B_T	Ip	Paux
ITER-FEAT									
a) Ref case	18.6/16.6	16.5/16.2	3.34	1.11/1.11	1.28/1.33	5.3/6.2	5.3	15	40
b) Gribov*	23.9	25.2	2.34	1.85/3.43	2.77/2.56	5.4/5.0	5.3	9	68
Fire									
a) Te, TI evl	10.1/10.2	9.8/10.2	2.75	1.06/1.06	1.33/1.40	3.0/3.7	10	7.7	20
b) Te, Ti, J evl	16.5	1.1	2.75	0.46	1.39	3.9/3.7	10	7.7	20
c) b+saw	8.3	8.1	2.75	1.00	1.33	3.1/3.7	10	7.7	20
IGNITOR									
a) with saw	9.1/13.1	86./12.0	2.74	1.00/1.01	1.24/1.22	11.2/10.9	13	11	10

ITER-FEAT AT based On DIII-D Results

- DIII-D H mode shot 106029 was used to determine an equilibrium suitable for Iter At scenarios, ref1
- For transport kinetic profiles consistent with the mhd properties of the scaled up equilibria are required. We assume suitable n_e near n_{Gw} , $T_e = T_i$ and solve the set of equations:

$$n_e - Z_{p1}n_{p1} - Z_{p2}n_{p2} - Z_{imp1}n_{imp1} - Z_{imp2}n_{imp2} = Z_b n_b + Z_\alpha n_\alpha \quad (4)$$

$$\begin{aligned} Z_{eff}n_e - \langle Z_{p1}^2 \rangle n_{p1} - \langle Z_{p2}^2 \rangle n_{p2} \\ - \langle Z_{imp1}^2 \rangle n_{imp1} - \langle Z_{imp2}^2 \rangle n_{imp2} = Z_b^2 n_b + Z_\alpha^2 n_\alpha \end{aligned} \quad (5)$$

$$\begin{aligned} n_e C_e T_e + n_{p1} C_i T_i + n_{p2} C_i T_i \\ + n_{imp1} C_i T_i + n_{imp2} C_i T_i = P - \frac{2}{3}(w_{beam} + w_\alpha) \end{aligned} \quad (6)$$

$$Z_{frac} n_{p1} - n_{p2} = 0 \quad (7)$$

$$Z_{impfrac} n_{p1} - n_{imp2} = 0 \quad (8)$$

APPLICATION: ITER-FEAT Weak Negative Central Shear Discharges

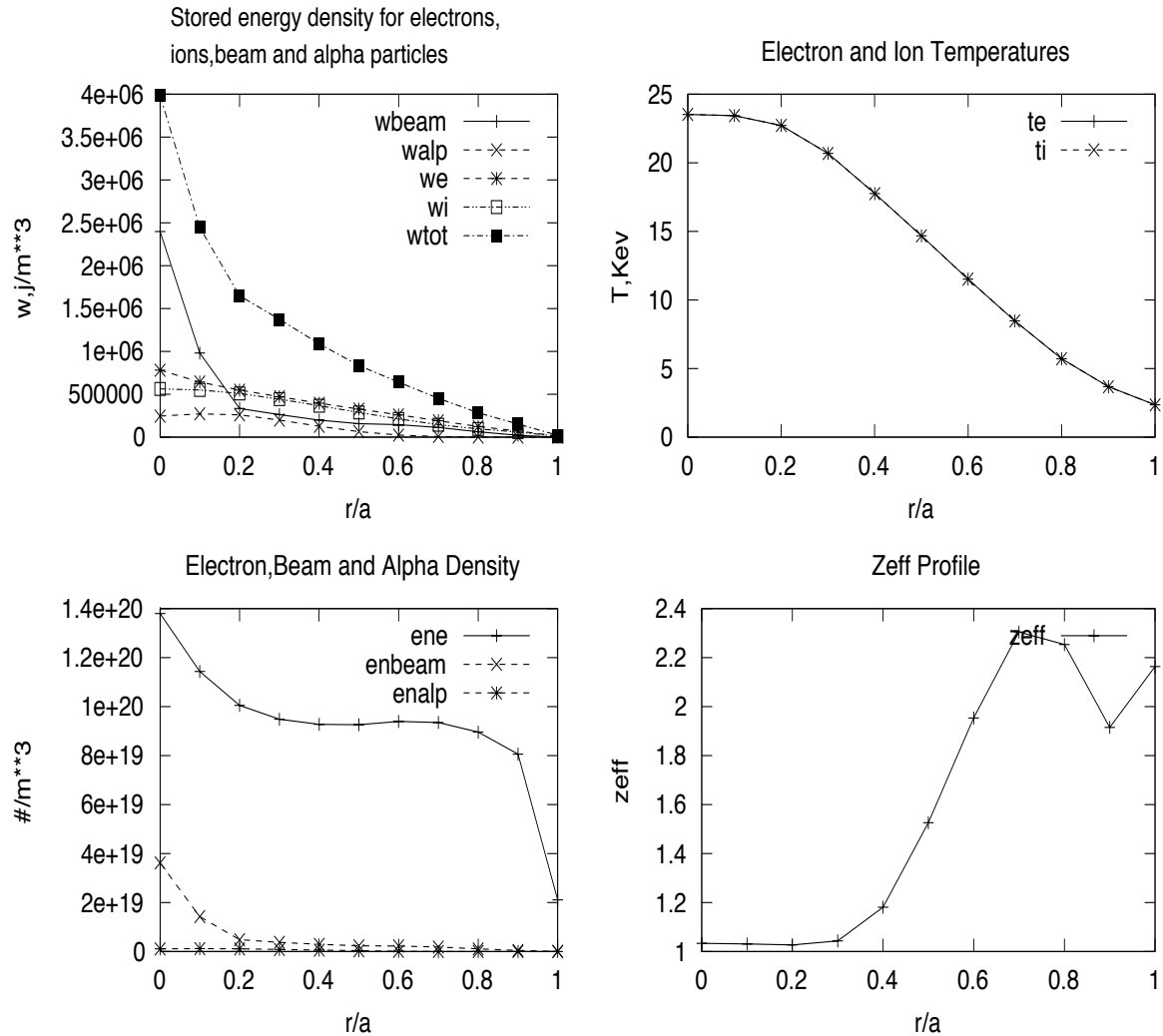


Fig. 1 Rho profiles used to deduce the electron temperature and primary and impurity ion densities as described in the text.

ITER-FEAT NBI

- We used 33MW of 1MEV negative ion injection and various amounts of simulated rf heating to investigate the confinement behavior.

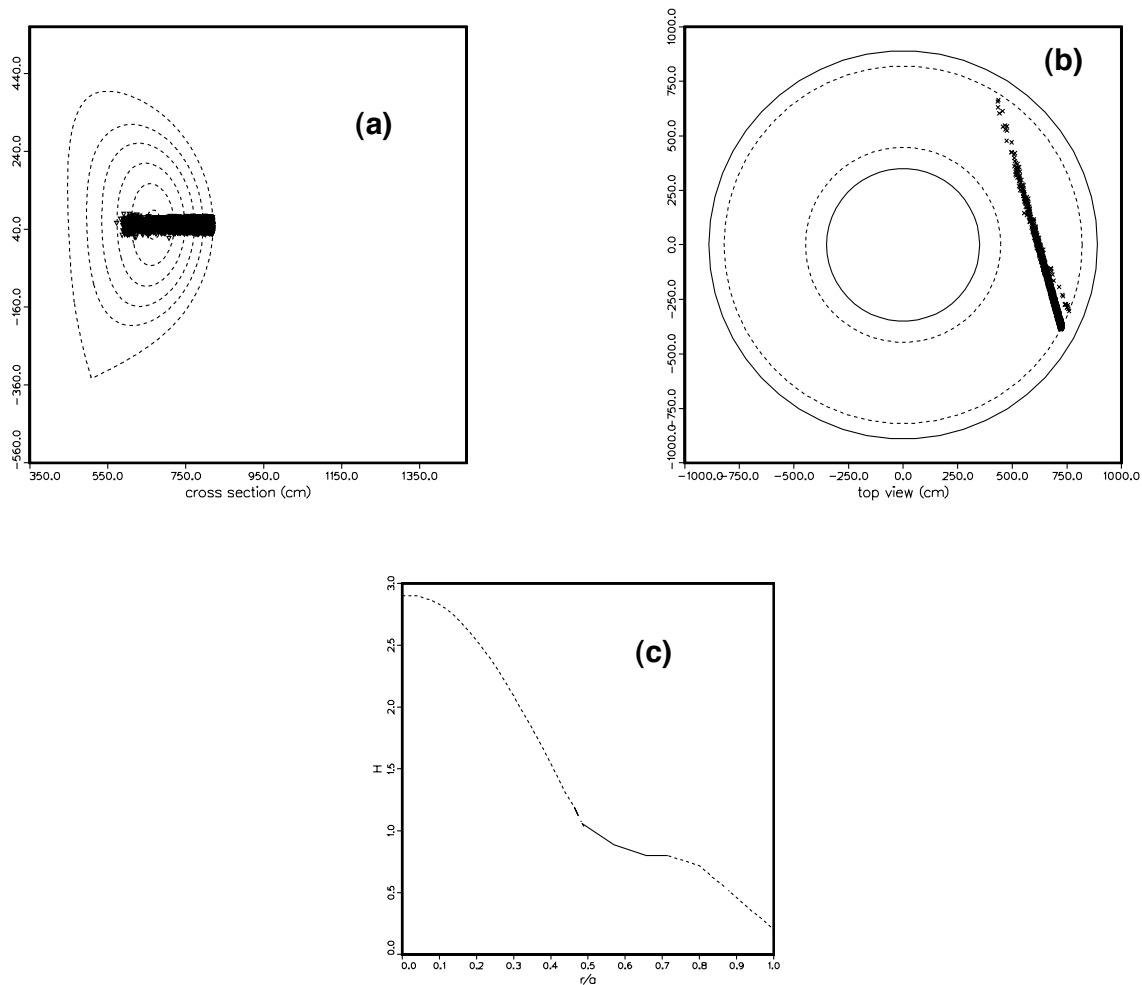
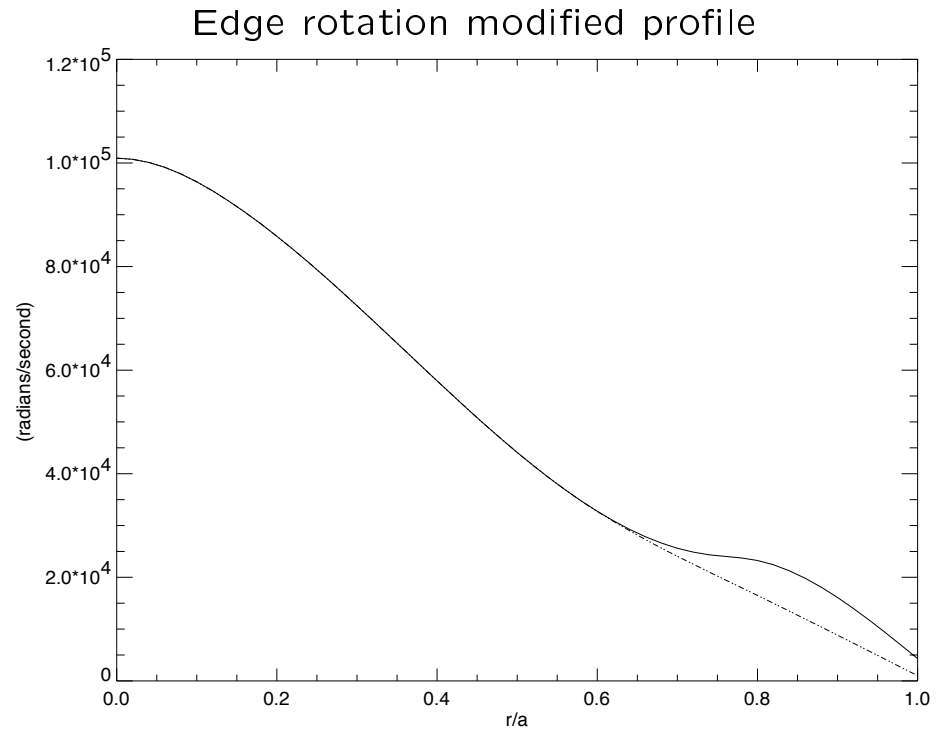
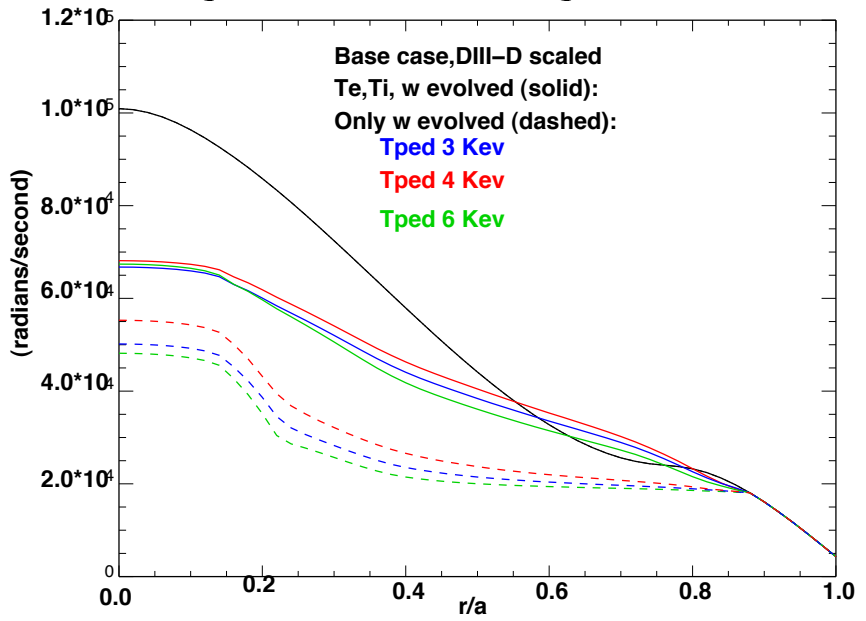


FIG : The neutral beam deposition , poloidal(a), toroidal (b). Prompt orbit averaged fast ion deposition (c).

APPLICATION: ITER-FEAT AT Weak Negative Central Shear Discharges

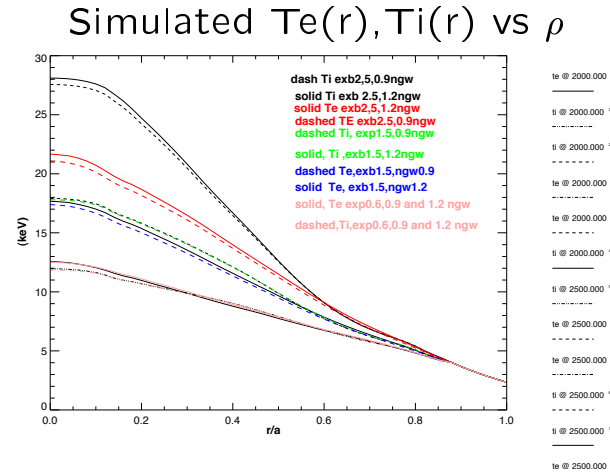
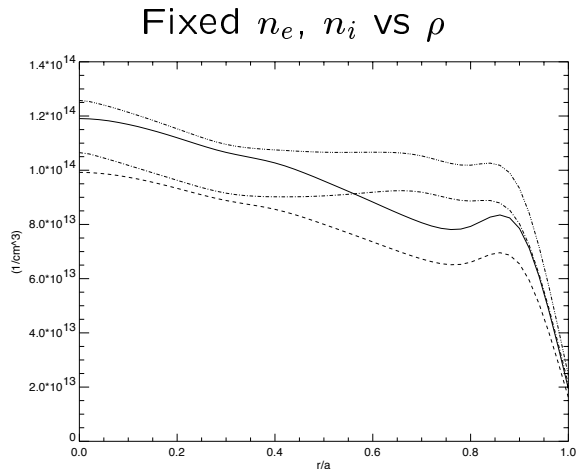
- $E \times B$ shear plays a central role in GLF23 discharges. Shown below are the toroidal rotation speed profiles obtained with GLF23 with and without evolving T_e, T_i and J for edge ("pedestal") temperatures of 3,4 and 6 Kev (see also Table 4). Modifying the edge toroidal rotational contribution to the shearing rate results in marginally improved confinement as is evident in Table 1. Resistive wall mode stabilization is expected for central rotation speeds greater than $1.e4$ rad/sec based on Mars calculations.

FIG 6: Toroidal rotation speed vs rho (1 Mev Tangential injection negative ion beam)

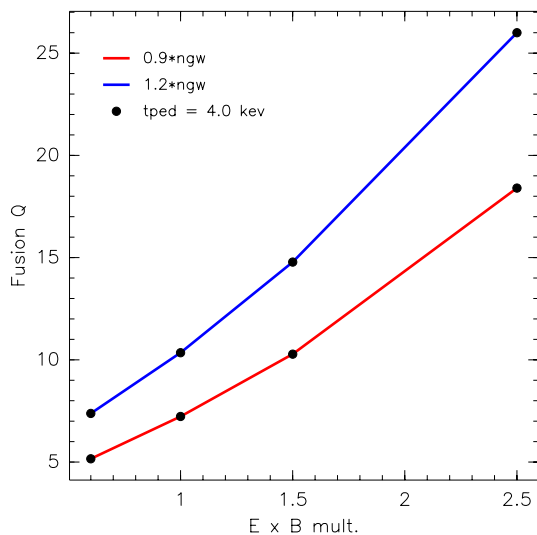


ITER-FEAT AT WNCS Discharges

- Increasing density to $1.2 \times n_{gw}$ does not change steady state temperatures significantly for $E \times B \leq 1.5$ ($T_{ped} = 4.0$ keV). Q and h89 improve, see below and Table 3.



Q vs $E \times B, N_{gw} = 0.9, 1.2$



$\beta_N H$ vs $E \times B, N_{gw} = 0.9, 1.2$

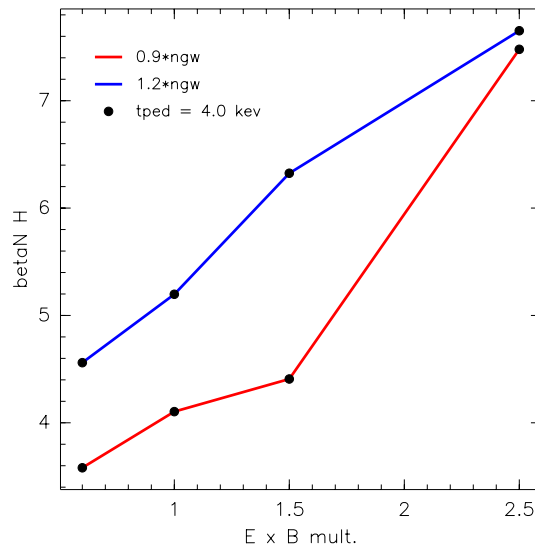


**TABLE 3: ITER-FEAT WNCs E X B
SCAN**

E x B	0.6	1.0	1.5	2.5
<i>0.9n_{gw}</i>				
Q	5.16	7.23	10.28	18.4
β_T	1.73	1.90	2.15	2.77
H89p	2.07	2.16	2.05	2.74
<i>1.2n_{gw}</i>				
Q	7.38	10.35	14.78	26.0
β_T	2.00	2.24	2.55	3.27
H89p	2.28	2.32	2.48	2.11
<i>lin ω</i>				
Q	5.36	8.3	12.3	21.85
β_T	1.73	2.0	2.31	3.03
H89p	2.09	2.17	2.05	2.72

**TABLE 4: ITER-FEAT WNCS T_{ped} Scan
With 33 Mw Beam**

T_{ped}, Kev	2.0	3.0	4.0	5.0	6.0
<i>0MWrf</i>					
<hr/> <hr/>					
<i>evolve : Te, Ti, J</i>					
$\omega = 0.2$ nom					
Q	NA	2.50	5.18	8.99	NA
β_T	NA	1.31	1.71	2.16	NA
H89p	NA	0.87	2.15	2.42	NA
$\omega = 0.6$ nom					
Q	NA	3.35	6.38	10.31	NA
β_T	NA	1.41	1.83	2.28	NA
H89p	NA	1.89	2.10	2.25	NA
$\omega = 1.0$ nom					
Q	1.74	4.05	7.38	11.58	15.58
β_T	1.07	1.48	1.91	2.38	2.81
H89p	1.52	1.86	2.10	2.56	2.66
<i>evolve : Te, Ti, J, ω</i>					
Q	NA	3.63	6.71	10.75	15.5
β_T	NA	1.44	1.86	2.31	2.79
H89p	NA	1.84	2.36	2.55	2.71
<i>66MWrf</i>					
<hr/> <hr/>					
<i>evolv : Te, Ti, J</i>					
Q	3.71	6.08	9.22	12.96	17.15
β_T	1.31	1.66	2.05	2.46	2.89
H89p	1.30	1.52	1.73	1.92	2.04

Summary, $T_{ped} = 6$ Kev Evolve T_e, T_i, J, ω

Minor radius a (cm):	186.4	b/a:	1.94
Nominal Rmajor (cm):	620.0	R at geom. cent. (cm):	635.3
R at mag. axis (cm):	673.8	Z at mag. axis (cm):	53.0
Volume (cm**3):	7.75E+08	Pol. circum. (cm):	1776.2
Bt (G):	5.30E+04	Ip (A):	9.92E+06
Bt at Rgeom (G):	5.17E+04	r(q = 1)/a:	0.00
Line-avg den (1/cm**3):	9.04E+13	Tau-particle-dt (s):	0.200
profiles	ucenter	uedge	ucen/uav
elec. den. (1/cm**3):	1.06E+14	2.11E+13	1.24
elec. temp. (keV):	19.82	3.52	2.03
ion temp. (keV):	20.69	3.52	2.02
current (A/cm**2):	65.96	71.63	1.32
Zeff:	1.04	2.16	0.58
q:	1.96	10.69	
q* at edge:		4.68	
ang. speed (1/sec):	6.76E+04	4.30E+03	2.26E+00
Neutron rate:	1.897E+20 #/s		
computed quantities			
Beam power elec. (W):	2.07E+07	ke at a/2 (1/cm-s):	2.12E+18
Beam power ions (W):	1.23E+07	ki at a/2 (1/cm-s):	4.02E+17
Beam power cx loss (W):	-2.63E+03	ki/kineo at a/2:	14.15
Shinethrough (%):	0.01	chi electrons at a/2:	2.34E+04
RF power absorbed:	0.00E+00	chi ions at a/2:	5.03E+03
Radiated power (W):	1.95E+07		
Poloidal B field (G):	7.02E+03	Beta-poloidal:	1.618
beam torque (nt-m)	4.49E+01	total torque (nt-m):	-4.28E+02
stored ang mtm (kg*m2/s):	3.56E+02	momt inertia (kg*m**2):	1.09E-02
	electrons	ions	thermal
Stored Energy (J)	1.618E+08	1.506E+08	3.125E+08
dE/dt (W):	8.904E+04	1.896E+05	2.786E+05
Input power (W):	1.029E+08		1.380E+08
Energy conf. time (s):	1.5740		2.2691
H(89p) =	2.71	betat	2.835E-02
Itot =	9.92E+06	Iohm =	3.69E+06
Iboot =	4.45E+06	Ibeam =	1.78E+06
QDD =	0.017797	QDT =	15.989103
		QTT =	0.029811

NTCC NUBEAM MODULES

- Nubeam is the neutral beam deposition and Monte Carlo fast ion physics package originally developed for Transp. Recently A.Pankin,D.McCune,and T.Ludescher encapsulated the Transp calculations and made them available for general use as an NTCC module.
- We are currently learning the Nubeam System by incorporating it into the Onetwo transport code.
- The system consists of an object based interface to the following modules:
 1. Xplasma (mhd related calculations)
 2. Preact (atomic and nuclear reaction rates)
 3. Nubeam (neutral beam deposition ,slowing down and thermal physics)
 4. Ezcdf (Netcdf interface)
 5. Pspline (various interpolation methods)

NTCC NUBEAM MODULES ...

- We have successfully built the NTCC package on Linux systems (Athlon and Xeon procesors) with pgf90 and lf95 at GA.
- Incorporation of the Nubeam system into Onetwo is currently about 50% complete

20: APS 2002, H.S.J.

Future Computational Enhancements

- Full Nubeam implementation in Onetwo with simple linear FPP solution added.
- Strong negative central shear GLF23 refined model.
- Refined neutral modeling with NTCC module NUT
- Time dependent eqdsk mode for rf codes Toray and NTCC Curaray module
- Direct coupling with Efit for kinetic/mhd profile analysis
- Computations optimized using both Open Mp and MPI